Structural Reassignment, Absolute Configuration, and Conformation of Hypurticin, a Highly Flexible Polyacyloxy-6-heptenyl-5,6-dihydro-2*H*-pyran-2-one†

José Alberto Mendoza-Espinoza,‡ Fabian López-Vallejo,‡,§ Mabel Fragoso-Serrano,§ Rogelio Pereda-Miranda,*,§ and Carlos M. Cerda-García-Rojas*,‡

Departamento de Química y Programa de Posgrado en Farmacología, Centro de Investigación y de Estudios Avanzados del Instituto Politécnico Nacional, A. P. 14-470, México, D. F. 07000 Mexico, and Departamento de Farmacia, Facultad de Química, Universidad Nacional Autónoma de México, Circuito Exterior Ciudad Universitaria, México, D. F. 04510 Mexico

Received July 19, 2008

The structural reassignment, absolute configuration, and conformational behavior of the highly flexible natural product hypurticin (pectinolide E), 6*S*-[3′*S*,5′*R*,6′*S*-triacetoxy-1*Z*-heptenyl]-5*S*-acetoxy-5,6-dihydro-2*H*-pyran-2-one (**1**), were ascertained by a molecular modeling protocol, which includes extensive conformational searching, geometry optimization by DFT B3LYP/DGDZVP calculations, and comparison between the theoretical (DFT) and experimental $^1H-^1H$ NMR coupling constants. Hyptolide (**2**), a related cytotoxic 5,6-dihydro-2*H*-pyran-2-one that increased the S phase of the HeLa cell cycle, was employed as a reference substance to validate the theoretical protocol designed to characterize the 3D properties of compound **1**. The related synthetic derivative, tri-*O*-acetyl-3,6-dideoxy-D-glucose diphenyldithioacetal (**14**), was prepared by a six-step reaction sequence starting from D-glucose and served as an enantiopure building block to reinforce the structural and configurational assignment of **1**. This protocol proved to be an important tool for the structural characterization of highly flexible bioactive polyoxygenated natural products.

Currently, chemical and pharmacological research are largely directed toward the discovery of new cytotoxic agents from natural sources.[1] Configurational and conformational behavior of bioactive principles requires an accurate description of their three-dimensional properties, thus permitting visualization and understanding of the possible interactions with target biomolecules.[2] For example, a relevant group of cytotoxic compounds, occurring in several members of the mint family (Lamiaceae), comprises polyacylated-6-heptenyl-5,6-dihydro-2*H*-pyran-2-ones[3] (e.g., **1**−**8**, Figure 1) containing an α,β-unsaturated δ-lactone known to bind protein thiol groups. This class of bioactive chemicals is structurally related to pironetin, an anticancer natural product, which selectively targets Lys-352 of α-tubulin.[4] Compounds such as hyptolide (**2**),[5] spicigerolide (**3**),[6] pectinolides A−C (**4**−**6**),[7] and 10-*epi*-olguine (**7**)[8] exhibit activity against specific tumor cell lines. However, the mechanism of action, the specific molecular target, the pharmacophore conformational requirements, and, in some cases, the absolute configuration of the stereogenic centers in the flexible side chain are not yet established, as in the case of the polyacylated chain of hypurticin (**1**), a natural 6-heptenyl-5,6-dihydro-2*H*-pyran-2-one. During the isolation of **1** from *Hyptis urticoides* by Romo de Vivar's group,[9] the C-6 absolute configuration was established as *S* by chiroptical measurements, the CD curve showing a positive Cotton effect similar to that of previously known 6-substituted-5,6-dihydro-α-pyrones[3,10] such as hyptolide (**2**)[5] and olguine (**8**).[11] The C-5 stereogenic center was assigned the *S* configuration due to the $J_{5,6}$ coupling constant, which evidenced the *cis* relationship between these hydrogens.[9] However, the absolute configuration of the stereogenic centers located at the heptenyl side chain was not elucidated. The variety of configurational possibilities and the high number of conformational arrangements arising from the flexibility of this molecular moiety precluded its full structural determination at that time.

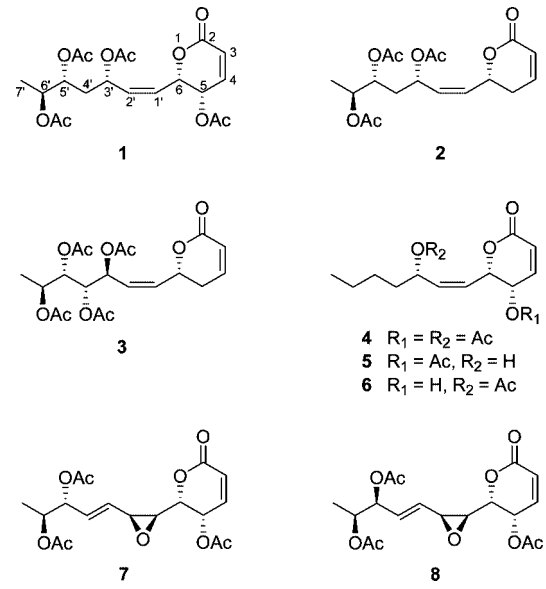

Figure 1. 6-Heptenyl-5,6-dihydro-2*H*-pyran-2-ones from Lamiaceae.

In the present investigation, a methodology involving the comparison between DFT and ^1H NMR coupling constants of flexible natural products was structured and applied to the configurational determination of the polyacylated chain of hypurticin (**1**). The DFT molecular modeling and coupling constant calculations for the four most likely stereoisomers of **1** (**1a**−**1d**), in comparison with the experimental coupling constant values, completed the configurational elucidation of the acyclic portion of hypurticin (**1**). This methodology was also applied to the flexible natural compound hyptolide (**2**) in order to study its conformational behavior. The established absolute configuration of **2**[5] served as a reliable reference to validate the theoretical protocols employed in this work. These calculations were subsequently used to select an appropriate natural hexose for the preparation of a representative enantiopure building block or chiral synthon (i.e., chiron[12]) for the

† Taken in part from the Ph.D. Thesis of J.A.M.-E. presented to Posgrado de la Sección Externa de Farmacología, CINVESTAV-IPN.

* To whom correspondence should be addressed. Tel: +52 55 5747 4035. Fax: +52 55 5747-7137. E-mail: ccerda@cinvestav.mx or pereda@servidor.unam.mx.

‡ Centro de Investigación y de Estudios Avanzados del Instituto Politécnico Nacional.

§ Universidad Nacional Autónoma de México.

10.1021/np800447k CCC: $40.75
Published on Web 03/05/2009

Table 1. ^{1}H NMR Data of Compounds **1**, **2**, and **14** Obtained by Nonlinear Fit of the Spectra to Spectral Parameters[a]

H	1	2	14[c]
3	6.24 (1H, d, $J_{3,4}$ = 10.50)	6.03 (1H, ddd, $J_{3,4}$ = 10.00, $J_{3,5\text{pro}R}$ = 1.00, $J_{3,5\text{pro}S}$ = 2.80)	
4	6.98 (1H, dd, $J_{3,4}$ = 10.50, $J_{4,5}$ = 5.60)	6.86 (1H, dddd, $J_{3,4}$= 10.00, $J_{4,5\text{pro}R}$ = 6.60, $J_{4,5\text{pro}S}$ = 2.40, $J_{4,1'}$ = −0.25)	
5[b]	5.32 (1H, dd, $J_{4,5}$ = 5.60, $J_{5,6}$ = 2.75)	2.38 (1H, ddddd, $J_{3,5\text{pro}R}$ = 1.00, $J_{4,5\text{pro}R}$ = 6.60, $J_{5\text{pro}R,5\text{pro}S}$ = −17.90, $J_{5\text{pro}R,6}$ = 3.90, $J_{5\text{pro}R,1'}$ = −0.50)	
5pro-*S*		2.45 (1H, dddd, $J_{3,5\text{pro}S}$ = 2.80, $J_{4,5\text{pro}S}$ = 2.40, $J_{5\text{pro}R,5\text{pro}S}$ = −17.90, $J_{5\text{pro}S,6}$ = 10.50)	
6	5.50 (1H, dddd, $J_{5,6}$ = 2.75, $J_{1',6}$ = 8.50, $J_{6,2'}$ = 0.80, $J_{6,3'}$ = −0.70)	5.20 (1H, ddd, $J_{5\text{pro}R,6}$ = 3.90, $J_{5\text{pro}S,6}$ = 10.50, $J_{6,1'}$ = 7.70)	
1′	5.78 (1H, dd, $J_{6,1'}$ = 8.50, $J_{1',2'}$ = 11.15)	5.76 (1H, ddddd, $J_{4,1'}$ = −0.25, $J_{5\text{pro}R,1'}$ = −0.50, $J_{6,1'}$= 7.70, $J_{1',2'}$ = 10.32, $J_{1',3'}$ = −0.40)	
2′	5.61 (1H, ddd, $J_{6,2'}$ = 0.80, $J_{1',2'}$ = 11.15, $J_{2',3'}$ = 9.65)	5.51 (1H, dd, $J_{1',2'}$ = 10.32, $J_{2',3'}$ = 9.50)	4.61 (1H, d, $J_{2',3'}$ = 3.25)
3′	5.48 (1H, dddd, $J_{6,3'}$ = −0.70, $J_{2',3'}$ = 9.65, $J_{3',4'\text{pro}R}$ = 7.25, $J_{3',4'\text{pro}S}$ = 5.85)	5.52 (1H, dddd, $J_{1,3'}$ = −0.40, $J_{2',3'}$ = 9.50, $J_{3',4'\text{pro}R}$ = 8.50, $J_{3',4'\text{pro}S}$ = 4.60)	5.24 (1H, ddd, $J_{2',3'}$ = 3.25, $J_{3',4'\text{pro}S}$ = 5.80, $J_{3',4'\text{pro}R}$ = 6.95)
4′pro-*R*	1.86 (1H, ddd, $J_{3',4'\text{pro}R}$ = 7.25, $J_{4'\text{pro}R,4'\text{pro}S}$ = −13.80, $J_{4'\text{pro}R,5'}$ = 2.75)	1.83 (1H, ddd, $J_{3',4'\text{pro}R}$ = 8.50, $J_{4'\text{pro}R,4'\text{pro}S}$ = −14.30, $J_{4'\text{pro}R,5'}$ = 2.90)	2.16 (1H, ddd, $J_{3',4'\text{pro}S}$ = 5.80, $J_{4'\text{pro}S,4'\text{pro}R}$ = −14.80, $J_{4'\text{pro}S,\ 5'}$ = 3.90)
4′pro-*S*	1.99 (1H, ddd, $J_{3',4'\text{pro}S}$ = 5.85, $J_{4'\text{pro}R,4'\text{pro}S}$ = −13.80, $J_{4'\text{pro}S,5'}$ = 8.20)	2.01 (1H, ddd, $J_{3',4'\text{pro}S}$ = 4.60, $J_{4'\text{pro}R,4'\text{pro}S}$ = −14.30, $J_{4'\text{pro}S,5'}$ = 9.60)	2.27 (1H, ddd, $J_{3',4'\text{pro}R}$ = 6.95, $J_{4'\text{pro}S,4'\text{pro}R}$ = −14.80, $J_{4'\text{pro}R,5'}$ = 8.10)
5′	4.96 (1H, ddd, $J_{4'\text{pro}R,5'}$ = 2.75, $J_{4'\text{pro}S,5'}$ = 8.20, $J_{5',6'}$ = 3.30)	4.90 (1H, ddd, $J_{4'\text{pro}R,5'}$ = 2.90, $J_{4'\text{pro}S,5'}$ = 9.60, $J_{5',6'}$ = 3.20)	5.01 (1H, ddd, $J_{4'\text{pro}S,5'}$ = 3.90, $J_{4'\text{pro}R,5'}$ = 8.10, $J_{5',6'}$ = 3.65)
6′	4.97 (1H, dq, $J_{5',6'}$ = 3.30, $J_{6',7'}$ = 6.25)	4.97 (1H, dq, $J_{5',6'}$= 3.20, $J_{6',7'}$= 6.37)	4.93 (1H, tq, $J_{5',6'}$ = 3.65, $J_{6',7'}$ = 6.45)
7′	1.22 (3H, d, $J_{6',7'}$ = 6.25)	1.20 (3H, d, $J_{6',7'}$= 6.37)	1.17 (3H, d, $J_{6',7'}$ = 6.45)

[a] Coupling constants in Hz. [b] Denoted as pro-*R* in **2**. [c] Phenyl groups appeared at δ 7.54−7.25 (10H, m). The configurational descriptors for pro-*R* H-4′ and pro-*S* H-4′ were inverted for direct comparative purposes.

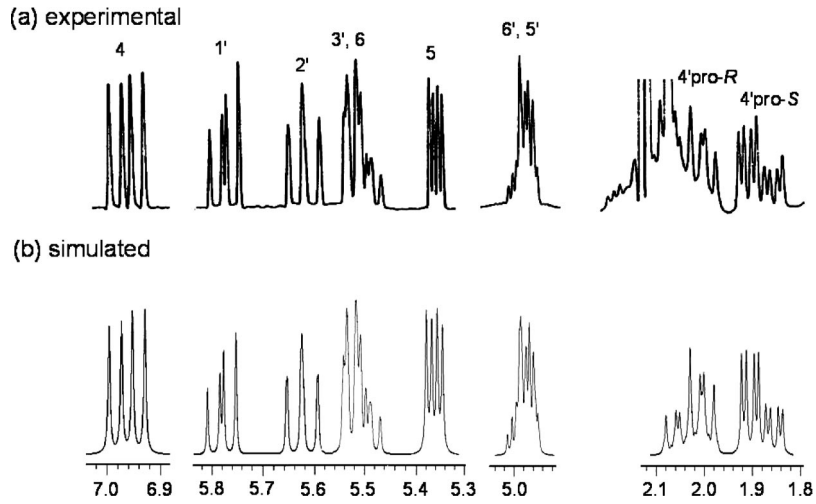

Figure 2. (a) Experimental and (b) simulated ^{1}H NMR spectrum of **1**.

acyclic portion of hypurticin (**1**) and hyptolide (**2**). The assignment of the correct absolute configuration of **1** is a crucial issue to achieve its total synthesis in order to further explore its biological potential. This exploratory situation for hypurticin (**1**) became mandatory as a consequence of the cytotoxicity[6,7] displayed for this class of 6-heptenyl-5,6-dihydro-2*H*-pyran-2-ones, as described here for the closely related hyptolide (**2**) and spicigerolide (**3**).

There are a few recent reports of the use of DFT calculated coupling constants for the configurational elucidation of inherently flexible natural products.[13] This approach constitutes an important tool for the structural characterization and conformational analysis of highly flexible polyoxygenated compounds. The procedure described here contributes to the enhancement of theoretical protocols recently applied to solve stereochemical aspects of natural products such as those based on optical rotation analysis,[14] vibrational[15] and electronic[16,17] circular dichroism, and chemical shift calculations.[18]

Results and Discussion

The similarity among **1** and the structurally related cytotoxic compounds **2**−**7**[5−8] was the starting point for the synthesis and evaluation of the biological properties of this 6-heptenyl-5,6-dihydro-2*H*-pyran-2-one. Due to the lack of an authentic sample of **1**, the experimental coupling constants were obtained through nonlinear fit of the spectrum to spectral parameters based on the original ^{1}H NMR plot for this compound.[19] This procedure permitted establishment of the chemical shifts and coupling constant values with a high degree of accuracy (Table 1). Analysis of these ^{1}H NMR data led to a reassessment of the position for one of the acetoxy groups in the heptenyl chain of hypurticin (**1**). The nonlinear fit of the spectrum of **1** to its spectral parameters using spectral simulation (Figure 2) was achieved with a root-mean-square deviation (rmsd) of 0.79 Hz. The analysis of ^{1}H−^{1}H vicinal coupling constants (Table 1) revealed that **1** bears the acetoxy groups at the C-3′, C-5′, and C-6′ positions and not at C-3′, C-4′, and C-6′ as previously reported.[9] The C-7 methyl group at δ 1.22 was coupled

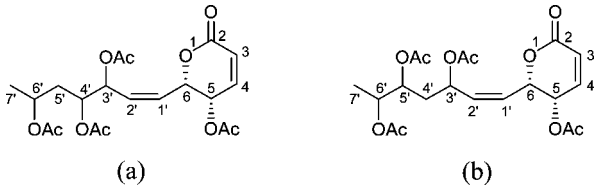

Figure 3. Modification of the structure of hypurticin based on nonlinear fit of the ^{1}H NMR spectrum to spectral parameters. (a) Originally proposed structure. (b) Revised structure.

with H-6′ (δ 4.97, $J_{6',7'} = 6.25$ Hz), which in turn was coupled with H-5′ and not with a methylene group (Figure 3). The signal for H-5′ appeared at δ 4.96 as a ddd coupled with H-6′ and with the C-4′ methylene protons. The pro-*R* H-4′ was observed at δ 1.86 as a ddd with $J_{3',4'proR} = 7.25$, $J_{4'proR,4'proS} = -13.80$ and $J_{4'proR,5'} = 2.75$ Hz, while the pro-*S* H-4′ appeared at δ 1.99 as a ddd with $J_{3',4'proS} = 5.85$, $J_{4'proR,4'proS} = -13.80$, $J_{4'proS,5'} = 8.20$ Hz. Both atoms were coupled with H-3′, which appeared as a dddd at δ 5.48 coupled with H-6, H-2′, pro-*R* H-4′, and pro-*S* H-4′ ($J_{6,3'} = -0.70$, $J_{2',3'} = 9.65$, $J_{3',4'proR} = 7.25$, $J_{3',4'proS} = 5.85$ Hz). The proximity in the chemical shifts for H-5′ and H-6′ could be the origin of the misinterpretation; however, the nonlinear fit of the spectrum method was conclusive in distinguishing between the two structural possibilities for **1**, as indicated in Figure 3. The experimental coupling constants matched those obtained for the simulated spectrum only when the $CH_3-CH-CH-CH_2-CH-CH=CH$ moiety instead of the $CH_3-CH-CH_2-CH-CH-CH=CH$ fragment was used for calculations and resulted in the reassignment of the C−C connectivities actually forming the polyacylated side chain. The ^{13}C NMR data of **1** were also in agreement with this modification, since the chemical shifts of the polyacylated chain (C-3′ at δ 66.7, C4′ at 34.9, C5′ at 71.0, C6′ at 70.5, and C7′ at 14.7) were very similar to the chemical shifts observed in the polyacylated chain of the related natural product hyptolide (**2**) (C-3′ at δ 66.3, C4′ at 34.6, C5′ at 70.7, C6′ at 70.2, and C7′ at 14.5), whose structure was secured by X-ray diffraction analysis.[5]

Once the overall structure of hypurticin (**1**) was revised, the next goal was the configurational assignment of the three stereogenic centers of the heptenyl moiety. A molecular modeling approach was initially achieved through calculation of the four most potentially adequate stereoisomers (**1a**−**1d**, Figure 4) based on the biogenetic assumption that the stereogenic center in the final portion of the chain at C-6′ has always been *S*.[3,6] Initially, each structure was modeled through a molecular mechanics systematic search protocol[20] and then followed by its optimization with density functional theory calculations. Certain premises were considered for these highly flexible substances to generate a rational number of conformations suitable for DFT calculations. The first was that by a systematic search procedure in which the three torsion angles C(2′)−C(3′)−C(4′)−C(5′), C(3′)−C(4′)−C(5′)−C(6′), and C(4′)−C(5′)−C(6′)−C(7′) in the side chain were varied by 120°; the number of possible conformers was established to be 27 after considering that all staggered arrangements[21] were started at +60° for each central bond. The second was that the most favorable synclinal geometry[22,23] for the acetoxy moieties began at H−C_{sp^3}−O−C_{sp^2} and C_{sp^3}−O−C=O dihedral angles of ca. 0° prior to the minimization procedure, but was left without any geometry restriction during the calculations. Also, conformational explorations for the acetyl groups were achieved within dihedral angle ranges of +60° to −60°. The third was that the starting geometry for the 5,6-dihydro-α-pyrone moiety, according to the observed $H_{5,6}$-coupling constant, was defined as having the pseudo-half-chair conformation of the lactone ring with atom C-6 out of the plane, the C-5 acetoxy group in a pseudo-axial orientation, and the heptenyl chain at C-6 in a pseudo-equatorial orientation.

These three assumptions established the initial series of the most stable conformers of **1a**−**1d**, which were then optimized through DFT calculation at the B3LYP/6-31G(d) level.[24] The smallest root-mean-square deviation obtained by comparison of the experimental ^{1}H−^{1}H vicinal coupling constants vs the calculated couplings for the four stereoisomers (Figure 4) provided an initial estimation in favor of the proper configurational arrangement. At this stage, the coupling constants were calculated from DFT dihedral angles through an empirically parametrized equation.[25,26] Structure **1a**, which corresponds to the 5*S*,6*S*,3′*S*,5′*R*,6′*S*-stereoisomer, showed the smallest difference between the calculated and observed values

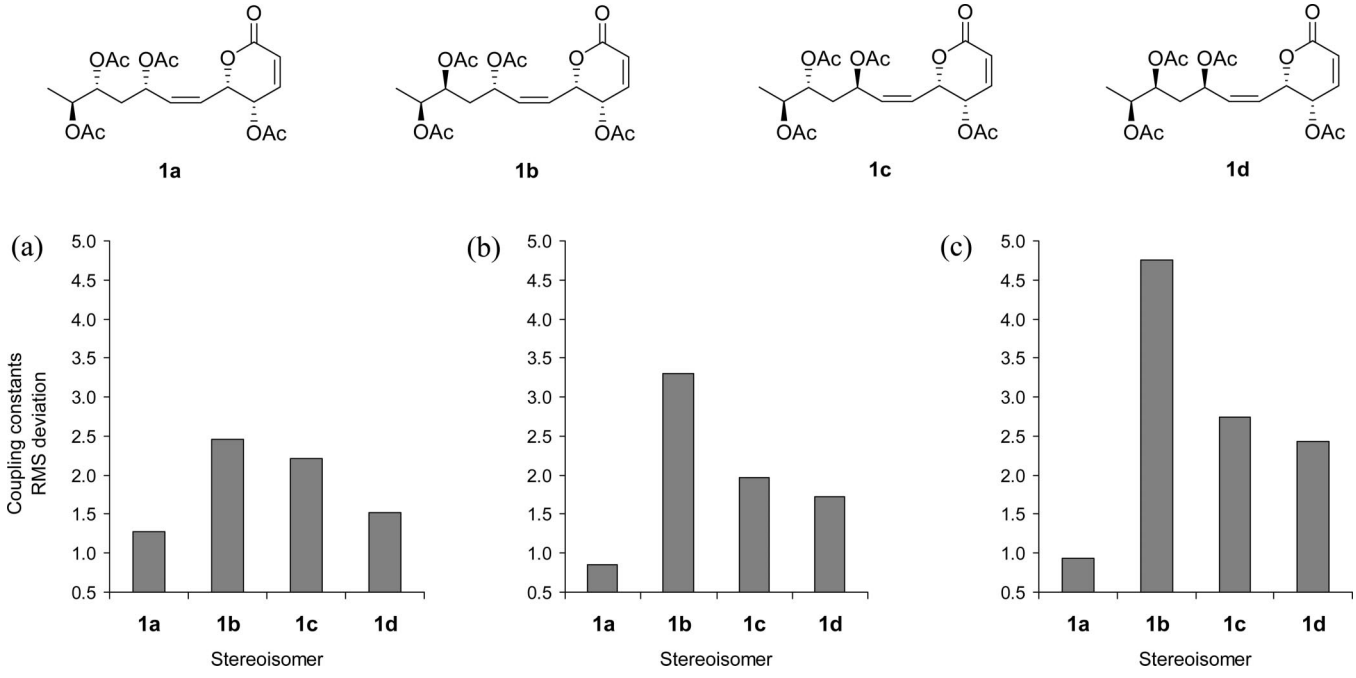

Figure 4. Root-mean-square deviations between DFT and experimental coupling constants of four possible hypurticin isomers (**1a**−**1d**) obtained (a) in a preliminary calculation with the DFT at B3LYP/6-31G(d) level of theory; (b) with an exhaustive conformational search and optimized at the B3LYP/DGDZVP level of theory; and (c) with an exhaustive conformational search optimized at the B3LYP/DGDZVP level and focusing on the polyoxygenated chain moiety.

Table 2. DFT B3LYP/DGDZVP Free Energies,[a] Population,[b] and Comparison between DFT and Experimental $^1H-^1H$ Coupling Constants[c] of Compound **1**

conformer	$\Delta G°$	P	$J_{3,4}$	$J_{4,5}$	$J_{5,6}$	$J_{6,1'}$	$J_{1',2'}$	$J_{2',3'}$	$J_{3',4'proS}$	$J_{3',4'proR}$	$J_{4'proS,5'}$	$J_{4'proR,5'}$	$J_{5',6'}$
1	0.000	17.698%	9.75	6.68	3.58	8.85	11.95	9.95	1.30	11.53	9.46	0.29	1.98
2	0.122	14.404%	9.78	6.68	3.96	9.56	12.08	10.34	1.09	10.60	9.95	0.35	2.06
3	0.259	11.430%	9.79	6.61	4.17	9.47	12.04	10.38	1.55	10.92	9.25	0.23	10.31
4	0.457	8.183%	9.81	6.10	3.55	10.24	12.24	7.06	11.81	1.38	1.36	6.38	11.12
5	0.616	6.267%	9.89	6.34	4.35	9.69	12.19	10.49	2.35	10.93	7.75	0.53	2.26
6	0.784	4.720%	9.75	6.69	3.95	5.99	11.82	10.46	12.07	1.60	3.33	11.07	8.41
7	0.961	3.501%	9.79	6.13	3.82	8.48	12.93	6.74	3.84	11.45	12.25	1.23	2.55
8	1.009	3.223%	9.75	6.62	4.37	5.45	12.07	10.30	12.68	3.40	5.03	12.12	2.13
9	1.020	3.169%	9.81	6.38	3.94	8.78	12.04	10.03	2.46	11.90	7.05	0.77	4.40
10	1.103	2.750%	9.81	6.12	3.83	8.76	12.79	6.87	5.09	10.83	12.94	2.72	2.47
11	1.146	2.558%	9.75	6.66	4.16	5.55	11.88	11.13	6.95	0.52	12.45	3.79	2.66
12	1.268	2.085%	9.77	6.47	4.70	5.54	12.39	11.00	5.92	2.65	3.95	12.66	1.99
13	1.276	2.054%	9.76	6.04	3.41	6.29	13.23	6.60	4.14	11.48	11.25	0.76	2.69
14	1.278	2.050%	9.74	6.63	3.97	5.77	11.90	10.62	12.18	3.88	6.71	0.74	2.70
15	1.281	2.036%	9.74	6.49	3.98	6.69	11.89	10.60	12.08	3.53	7.77	0.29	10.46
16	1.297	1.982%	9.80	6.03	3.62	10.45	12.32	7.58	3.81	12.17	10.26	0.65	10.13
17	1.340	1.843%	9.78	6.07	3.50	9.12	12.29	10.88	1.91	5.81	7.76	0.48	2.24
18	1.419	1.613%	9.80	6.22	4.02	6.39	12.01	10.84	10.08	0.52	2.36	4.97	11.17
19	1.444	1.547%	9.79	6.15	3.74	7.97	11.77	10.40	12.99	2.10	0.19	9.49	2.55
20	1.632	1.128%	9.71	6.27	3.03	5.18	13.34	7.41	2.59	5.78	10.95	0.61	1.81
21	1.715	0.979%	9.77	6.68	3.90	9.72	11.72	10.60	4.66	11.21	4.85	2.61	11.03
22	1.859	0.768%	9.71	6.57	3.56	2.27	13.67	10.51	3.67	11.03	11.96	11.30	2.54
23	2.090	0.520%	9.81	6.17	3.74	7.01	11.74	10.24	12.68	2.22	3.39	11.88	0.48
24	2.175	0.450%	9.84	6.22	4.28	8.72	12.27	7.38	13.69	3.89	5.81	11.68	2.24
25	2.194	0.436%	9.66	6.58	3.20	4.50	13.45	6.91	13.17	4.30	5.01	12.09	2.10
26	2.393	0.312%	9.86	6.10	3.88	9.56	13.35	5.33	3.96	4.03	2.22	12.09	1.41
27	2.450	0.283%	9.69	6.57	3.31	4.54	13.47	6.88	12.76	4.50	6.98	0.53	1.55
28	2.536	0.245%	9.71	6.23	2.91	5.15	13.39	7.55	5.31	3.02	3.91	12.81	2.00
29	2.567	0.232%	9.82	6.10	3.67	10.20	12.05	7.03	12.87	3.95	7.73	4.44	2.56
30	2.587	0.225%	9.69	6.55	3.57	2.27	13.62	10.67	3.56	11.37	11.04	0.85	10.14
31	2.617	0.214%	9.83	6.11	3.60	9.78	12.19	7.01	13.61	3.41	5.65	11.67	2.36
32	2.695	0.187%	9.66	6.65	2.91	3.35	13.56	9.62	4.39	11.83	10.91	0.60	2.55
33	2.720	0.180%	9.69	6.59	3.31	4.28	13.71	7.44	2.71	5.66	10.13	0.49	10.42
34	2.732	0.176%	9.70	6.56	3.38	4.49	13.48	7.49	2.53	5.84	10.76	0.54	1.83
35	2.758	0.168%	9.79	6.39	4.59	5.54	12.39	11.00	5.92	2.65	3.95	12.66	4.09
36	2.858	0.142%	9.65	6.63	3.12	4.03	13.59	8.29	12.10	2.25	1.95	5.99	11.01
37	2.895	0.134%	9.83	6.13	3.84	9.09	12.60	7.90	4.99	11.92	4.10	3.20	11.07
38	3.024	0.107%	9.70	6.51	3.53	6.08	12.95	9.19	2.14	5.70	8.79	0.39	2.33
	averaged values[d]		**9.78**	**6.48**	**3.87**	**8.42**	**12.18**	**9.60**	**4.83**	**8.17**	**7.91**	**2.82**	**4.82**
	experimental[e]		**10.50**	**5.60**	**2.75**	**8.50**	**11.15**	**9.65**	**5.85**	**7.25**	**8.20**	**2.75**	**3.30**

[a] In kcal/mol. [b] In percent from $\Delta G°$ values at 298 K and 1 atm. [c] In Hz calculated from the B3LYP/DGDZVP structures. [d] $\sum_i J_i \times P_i$, where J_i is the coupling constant value for each conformer and P_i is the population for the ith conformation. [e] Obtained by nonlinear fit of the spectrum to spectral parameters.

(rmsd = 1.27). However, in order to refine the computational approach for making a clearer visualization of the differences among the four stereoisomers (**1a**−**1d**), they were subjected to an exhaustive conformational search and geometrical optimization at a higher level of theory. Thus, in addition to the initial rotation by 120° of the torsion angles of the C(3′)−C(4′)−C(5′)−C(6′) fragment, the C(1′)═C(2′)−C(3′)−C(4′) and C(5)−C(6)−C(1′)═C(2′) dihedral angles were rotated in steps of 180°, generating a total of four series of 27 conformers. This systematic search afforded 108 conformers for each stereoisomer (**1a**−**1d**). For **1a**, a total of 19 structures were discarded because of the presence of very large hindering steric effects, partial atomic overlapping, or a relative MMFF energy[27] higher than 10 kcal mol^{-1}. The remaining 89 conformers were geometrically optimized at the B3LYP/DGDZVP level,[28] and the calculation of their vibrational frequencies and thermodynamic parameters was carried out at 298 K and 1 atm. Table 2 lists the relative free energies as well as the Boltzmann distribution for the 38 most relevant conformers, which fell within a $\Delta G°$ range of between 0 and 3.3 kcal mol^{-1}, offering evidence of the high flexibility of this structure. The conformational population was estimated according to the $\Delta G° = -RT \ln K$ equation, taking into consideration a cyclic equilibrium between the 38 selected conformers, which yielded $K_{1,2} = n_2/n_1$, $K_{2,3} = n_3/n_2$,... $K_{38,1} = n_1/n_{38}$ and $n_1 + n_2 + n_3 + ... + n_{38} = 1$. In these equations, $K_{i,j}$ denotes the equilibrium constants and n_i the number of moles.

Because $^1H-^1H$ NMR coupling constants are highly sensitive to geometrical and conformational changes, both the configuration and conformation of flexible molecules can be validated if there is agreement between experimental and theoretical $^3J_{HH}$ values.[6] Accordingly, the theoretical $^3J_{HH}$ coupling constants were calculated[29] (Table 2) using the NMR protocols as implemented in the Gaussian 03 software, which employed the gauge including atomic orbitals (GIAO) method[30] for computation of the magnetic shielding tensors at the DFT B3LYP/DGDZVP level. Application of this relatively new approach in natural compounds has afforded excellent results.[31] Each coupling value was Boltzmann-weighted taking into account the DFT population to integrate the population-averaged coupling constants, and these calculated total values were contrasted with the experimental data obtained by nonlinear fit of the spectrum to spectral parameters, as shown in Figure 2, where the experimentally previously reported[19] ^1H NMR plot of **1** is compared with its simulated trace. The close match between the two NMR spectra shown in Figure 2 (rmsd = 0.79 Hz) and between the calculated and observed coupling constants listed in Table 2 (rmsd = 0.85 Hz) indicated that the conformations and populations of compound **1** in $CDCl_3$ solution are quite similar to those found in the DFT molecular models and confirm the proposed 5*S*,6*S*,3′*S*,5′*R*,6′*S* configuration for hypurticin (**1**). In contrast, the same procedure was applied to stereoisomers **1b**−**1d** yielding 14, 11, and 20 relevant conformers, which are listed in Tables S1−S3 (Supporting Informa-

Table 3. Comparison between the Experimental Vicinal Coupling Constants for the Heptenyl Chain of Compound **1** and the DFT-Calculated Values of Stereoisomers **1a**−**1d**[a]

coupling	experimental	**1a**	**1b**	**1c**	**1d**
$J_{6,1'}$	8.50	8.42	6.70	10.17	9.47
$J_{1',2'}$	11.15	12.18	11.78	11.73	11.66
$J_{2',3'}$	9.65	9.60	10.35	10.48	9.96
$J_{3',4'proS}$	5.85	4.83	**11.63**	**2.93**	7.42
$J_{3',4'proR}$	7.25	8.17	**3.38**	**11.19**	6.77
$J_{4'proS,5'}$	8.20	7.91	**4.72**	**11.80**	**4.71**
$J_{4'proR,5'}$	2.75	2.82	**9.97**	2.58	**6.57**
$J_{5',6'}$	3.30	4.82	3.61	4.18	3.26

[a] In Hz. The coupling constants printed in boldface for **1b**−**1d** show noticeable differences with the experimental values.

tion). Comparison between the Boltzmann-weighted DFT-calculated vicinal coupling constants and the experimental data (Figure 4b) showed a much higher rmsd (3.30 for **1b**, 1.97 for **1c**, and 1.72 Hz for **1d**) compared to stereoisomer **1a** (0.85 Hz). If the rmsd analysis is focused on the vicinal couplings of the polyoxygenated chain moiety, where the configurational changes actually take place, the rmsd is substantially increased to 4.75 for **1b**, 2.75 for **1c**, and 2.43 Hz for **1d** (Figure 4c), resulting in a clear discernment of the proper configuration for compound **1**. Table 3 summarizes the vicinal coupling constants for the heptenyl chain of stereoisomers **1a**−**1d**, reflecting the degree of accuracy and differences resulting by application of this methodology. While the DFT-calculated couplings for stereoisomer **1a** essentially matched the experimental values, several coupling constants of **1b**−**1d**, printed in bold-face type in Table 3, showed noticeable differences, allowing the elimination of these stereoisomers.

Figure 5 shows the eight most relevant conformers of **1** accounting for ca. 70% of the population. In the global minimum (**1**-*1*) and the second minimum (**1**-*2*) there is spatial proximity (2.24 and 2.36 Å) between H-5 and the carbonyl group of the acetoxy moiety at C-5′, suggesting the presence of a weak hydrogen bond.[32,33] In fact, this phenomenon seems to be present in many minimum energy structures contributing to stability and, to some extent, directing the conformational behavior of the polyacylated 6-heptenyl-5,6-dihydro-2*H*-pyran-2-ones.

In order to obtain additional data in relation to this phenomenon, the DFT-coupling constants methodology was applied to hyptolide (**2**). Although the absolute configuration of hyptolide (**2**) was established,[5] the DFT-coupling constants approach was also applied to this natural product in order to evaluate the accuracy of the protocol and to estimate the degree of deviation between the two sets of coupling constants. As a consequence of this analysis, the conformational behavior of natural product **2** was explored for the first time. From the group of 108 conformers arising from a procedure identical to that applied to compound **1**, 25 structures were discarded. The 83 most stable conformers were optimized at the B3LYP/DGDZVP level,[28] and calculation of the vibrational frequencies and thermodynamic parameters were also carried out. Table 4 shows the relative free energies and the Boltzmann distribution for the 28 conformers, which all fall within a $\Delta G°$ value between 0.0 and 3.3 kcal mol^{-1}, indicating that the conformational dispersion in hyptolide (**2**) was not as broad as that of hypurticin (**1**). Figure 6 contains the eight most populated conformers for hyptolide (**2**), which in all cases exhibit the presence of weak hydrogen bonds[32,33] within a range between 2.40 and 2.58 Å. The dihydropyrone ring exhibits more conformational variants than those in **1**, which could be due to the absence of the C-5′ acetoxy moiety, thus reducing the steric effect. The rmsd between the experimental and DFT-calculated couplings for the 28 most stable conformations was 0.94 Hz. Therefore, the accuracy of the models was assured. Iterative spectral simulation was employed to measure the experimental coupling constants of **2** with an rmsd of 0.87 Hz (Supporting Information, Figure S1). From these calculations it was clear that

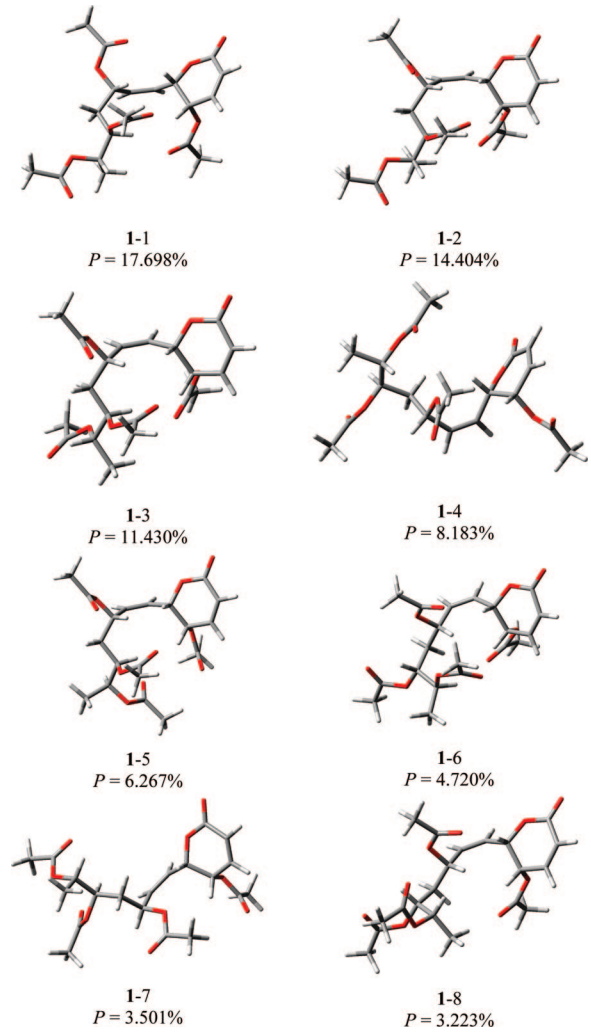

Figure 5. The eight most relevant conformers of **1** accounting for ca. 70% of the population.

the structure and the absolute configuration of hypurticin (**1**) at C-3′, C-5′, and C-6′ was identical to that described for hyptolide (**2**).

In order to chemically corroborate the absolute configuration for the stereogenic centers located at the heptenyl residue of hypurticin (**1**), the carbohydrate derivative tri-*O*-acetyl-3,6-dideoxy-D-glucose diphenyldithioacetal (**14**) was prepared as a simple flexible model with the same relative configuration presumably present in the acyclic moiety of **1**. Furthermore, **14** represents a chiron for the preparation of *ent*-hypurticin (*ent*-**1**) as well as providing an economical building block for its utilization in the synthesis of enantiomeric compound **1**, substituting expensive *ent*-glucose needed as the enantiopure template to achieve the total synthesis of hypurticin (**1**) and hyptolide (**2**). Preparation of tri-*O*-acetyl-3,6-dideoxy-D-glucose diphenyldithioacetal (**14**) was carried out by selective 3,6-dideoxygenation of α-methyl D-glucoside (**9**) through a tetratosylate intermediate (**10**)[34] followed by reduction with LAH to yield derivative **11**. Deprotection of **11** with 1.0 N HCl afforded paratose (**12**),[35,36] which upon protection with benzenethiol in $BF_3 \cdot Et_2O$ gave diphenyldithioacetal **13**. Acetylation of **13** using Ac_2O in pyridine (Scheme 1) yielded compound **14**. The correlation between the experimental $^1H-^1H$ vicinal coupling constants of **1** and the experimental values for the flexible model **14** (Figure 7), both obtained by nonlinear fit of the spectrum to spectral parameters with an rmsd of 0.32 Hz (Supporting Information, Figure S2), provided additional support for the configuration of compound **1**. The NMR assignments were supported by the information provided by 2D NMR experiments. The $^1H-^1H$ COSY spectrum of **1** showed the corresponding cross-peaks that were useful to verify the atom

Table 4. DFT B3LYP/DGDZVP Free Energies,[a] Population,[b] and Comparison between DFT and Experimental $^1H-^1H$ Vicinal Coupling Constants[c] of Compound **2**

conformer	$\Delta G°$	P	$J_{3,4}$	$J_{4,5S}$	$J_{4,5R}$	$J_{5S,6}$	$J_{5R,6}$	$J_{6,1'}$	$J_{1',2'}$	$J_{2',3'}$	$J_{3',4'proS}$	$J_{3',4'proR}$	$J_{4'proS,5'}$	$J_{4'proR,5'}$	$J_{5',6'}$
1	0.000	29.905%	9.86	2.20	6.83	12.01	3.93	10.15	11.66	10.47	1.88	11.14	9.94	0.28	1.93
2	0.205	21.158%	9.87	2.20	6.82	11.99	3.95	10.13	11.69	10.44	1.81	11.14	9.84	0.30	10.36
3	0.406	15.070%	9.85	2.25	6.84	12.34	3.94	10.22	11.77	10.07	2.57	11.14	10.78	0.50	2.60
4	0.864	6.956%	9.83	2.25	6.86	12.39	3.78	10.22	11.81	10.60	2.97	11.10	12.02	1.08	2.43
5	1.078	4.847%	9.83	2.37	6.80	12.89	3.82	6.14	12.24	9.20	12.55	3.67	7.07	0.49	1.67
6	1.242	3.675%	9.83	2.37	6.83	12.82	3.69	6.08	12.25	9.24	12.88	3.65	5.11	12.12	2.20
7	1.632	1.903%	9.81	2.37	6.86	13.04	3.66	4.93	12.90	10.09	3.81	11.72	11.55	0.74	1.57
8	1.650	1.846%	9.86	2.18	6.73	13.16	4.19	7.27	11.72	10.25	12.60	2.13	2.54	10.81	9.51
9	1.673	1.775%	9.84	2.36	6.78	12.87	3.82	6.15	12.52	9.79	3.13	4.81	9.30	0.33	2.74
10	1.748	1.564%	9.81	2.38	6.87	13.27	3.75	4.67	12.91	10.19	4.67	11.60	11.58	1.18	10.08
11	1.841	1.337%	9.83	2.35	6.78	12.85	3.78	6.14	12.49	9.96	2.87	5.25	10.30	0.37	1.93
12	1.848	1.321%	9.84	2.36	6.78	12.87	3.80	6.13	12.57	9.89	3.09	4.93	8.89	0.27	2.99
13	1.881	1.250%	9.82	2.26	6.66	12.31	3.82	10.42	12.22	7.55	3.69	12.08	10.47	0.74	10.13
14	1.961	1.092%	9.84	2.24	6.63	12.27	3.80	9.28	12.81	6.70	3.40	11.58	11.48	0.87	2.55
15	2.052	0.936%	9.85	2.25	6.68	13.22	4.04	7.82	11.73	10.61	11.71	1.72	1.43	6.38	11.06
16	2.089	0.880%	9.81	2.36	6.87	13.18	3.68	4.83	12.87	10.18	4.46	11.50	11.88	0.94	2.31
17	2.121	0.833%	9.79	2.36	6.83	12.83	3.55	5.55	12.73	10.08	11.23	1.40	2.08	5.56	11.10
18	2.382	0.536%	9.82	2.38	6.77	12.88	3.76	6.37	12.36	9.35	12.18	4.43	7.46	0.30	10.37
19	2.407	0.514%	9.86	2.25	6.63	12.24	3.85	9.74	12.48	7.09	4.97	10.79	12.84	2.60	2.47
20	2.549	0.405%	9.87	2.20	6.78	12.46	4.14	9.48	11.53	10.01	4.46	11.38	4.81	2.58	10.95
21	2.589	0.378%	9.87	2.22	6.66	13.13	4.08	7.66	11.70	10.08	12.86	3.60	5.78	11.53	2.35
22	2.667	0.332%	9.91	2.39	6.66	12.85	3.97	6.63	12.17	12.17	12.88	3.15	3.67	10.89	9.80
23	2.678	0.326%	9.87	2.38	6.71	12.93	3.99	6.61	12.12	8.84	12.34	4.77	6.11	0.90	2.99
24	2.704	0.312%	9.84	2.35	6.79	12.88	3.77	6.04	12.53	9.89	5.23	3.10	4.27	12.81	1.96
25	2.727	0.300%	9.85	2.23	6.64	12.57	3.80	9.35	12.18	10.61	2.35	5.13	8.20	0.40	2.42
26	2.818	0.257%	9.84	2.35	6.79	12.84	3.81	6.04	12.65	9.99	3.07	5.01	9.19	0.23	10.37
27	3.103	0.159%	9.80	2.37	6.80	12.79	3.59	6.02	12.53	9.30	12.81	3.23	3.55	11.81	0.76
28	3.211	0.132%	9.86	2.26	6.72	12.26	3.80	9.95	12.02	6.92	13.57	3.40	5.45	11.77	2.31
	averaged values[d]		**9.85**	**2.25**	**6.82**	**12.32**	**3.89**	**9.20**	**11.89**	**10.15**	**3.77**	**9.74**	**9.56**	**1.54**	**4.55**
	experimental[e]		**10.00**	**3.00**	**6.00**	**12.00**	**3.00**	**8.34**	**10.32**	**9.50**	**4.60**	**8.50**	**9.60**	**2.90**	**3.30**

[a] In kcal/mol. [b] In percent from $\Delta G°$ values at 298 K and 1 atm. [c] In Hz calculated from the B3LYP/DGDZVP structures. [d] $\sum_i J^i \times P^i$, where J^i is the coupling constant value for each conformer and P^i is the population for the ith conformation. [e] Obtained by nonlinear fit of the spectrum to spectral parameters.

sequence in the triacylated chain. Thus, the H-2′ doublet at δ 4.61 displayed a cross-correlation with H-3′ at δ 5.24, which in turn showed correlations with the methylene hydrogens pro-*R* H-4′ and pro-*S* H-4′ at δ 2.16 and 2.27, respectively. Both atoms displayed correlations with H-5′ (δ 5.01), which was coupled with H-6′ (δ 4.93). Finally, H-6′ displayed an intense cross-correlation with the C-7′ methyl group (δ 1.17). The ^{13}C NMR signals of **1** were assigned via the $^{13}C-^1H$ HETCOR plot, which was useful to distinguish the signals for the methine carbons C-2′ (δ 61.9), C-3′ (δ 72.1), C-5′ (δ 71.3), and C-6′ (δ 70.2), which showed cross-correlations with H-2′ (δ 4.61), H-3′ (δ 5.24), H-5′ (δ 5.01), and H-6′ (δ 4.93), respectively. A similar chemical model, the diphenyldithioacetal derivative of L-mannose, was previously used in the stereochemical elucidation of spicigerolide (**3**), whose total synthesis was successfully achieved.[6]

The DFT-coupling constant method *per se* is unable to distinguish between a pair of enantiomers. In order to further support the absolute configuration of hypurticin (**1**), the DFT optical rotations at the sodium D-line[14,37,38] for the 38 most relevant conformers of **1** were calculated (Table S4) using the B3LYP/DGDZVP geometrically optimized structures. Boltzmann-weighting of the optical rotations afforded the averaged theoretical value $[\alpha]_D = +199.6$, which was in agreement with the dextrorotatory published value for hypurticin (**1**) ($[\alpha]_D = +175$).[9] According to the equation $\Delta[\alpha]_D = [\alpha]_D(\text{calc}) - [\alpha]_D(\text{expt})$,[38] compound **1** gives a $\Delta[\alpha]_D$ value of only +24.4, while its corresponding enantiomer (*ent*-**1**) gives a much larger $\Delta[\alpha]_D$ value in absolute terms (−374.6). All these results point out that the absolute configuration for hypurticin (**1**) is in fact 6*S*-[3′*S*,5′*R*,6′*S*-triacetoxy-1*Z*-heptenyl]-5*S*-acetoxy-5,6-dihydro-2*H*-pyran-2-one. As a consequence of this revision, the structure of hypurticin (**1**) actually corresponds to that of pectinolide E, recently isolated from *Hyptis pectinata*.[39]

The cytotoxicity of hyptolide (**2**) and spicigerolide (**3**) was evaluated against human laryngeal epidermoid carcinoma cells (HEp-2), nasopharyngeal cancer cells (KB), and cervical cancer (HeLa) cells. As indicated in Table 5, hyptolide (**2**) is more potent than spicigerolide (**3**) in the three tested cell lines. Hyptolide (**2**) displayed the highest activity against HeLa cells, while spicigerolide (**3**) showed selectivity against nasopharyngeal cancer cells (KB). In order to obtain information for the mechanism of cytotoxic action of polyacylated-6-heptenyl-5,6-dihydro-2*H*-pyran-2-ones, a cell cycle progression was studied by flow cytometry employing the cervical cancer (HeLa) cell line. The distribution of DNA content in the cell population was analyzed by this technique, showing that after 48 h of exposure to hyptolide (**2**) a moderate S-phase arrest was observed, as reflected by an increment from 42 to 57% of the cell population in this phase and a decreased proportion of cells in G1 and G2 phases (Table 6). In contrast, spicigerolide (**3**) showed a significant G2-phase arrest, evidenced by the increment of this phase from 14 to 23%. The basis for the difference in their effects on the cell cycle is unknown and deserves further attention. Detailed studies are also needed in relation to the modulatory effects associated with the configurational changes in the flexible polyoxygenated side chain and the cytotoxic potential of the alkylating 5,6-dihydro-2*H*-pyran-2-one nucleus.

In conclusion, the molecular modeling protocols may be useful in predicting the absolute configuration and to closely describe the conformation of highly flexible natural products such as **1** and **2**, as well as application to other cytotoxic polyacylated-6-heptenyl-5,6-dihydro-2*H*-pyran-2-ones[40] to accurately select the appropriate sugar-based chiron as enantiopure building blocks[6] for their total synthesis in order to guarantee that the absolute configuration of the synthetic product will be identical to that of the natural substance.

Experimental Section

General Experimental Procedures. Optical rotations were measured in $CHCl_3$ on a Perkin-Elmer 241 polarimeter. IR spectra were obtained

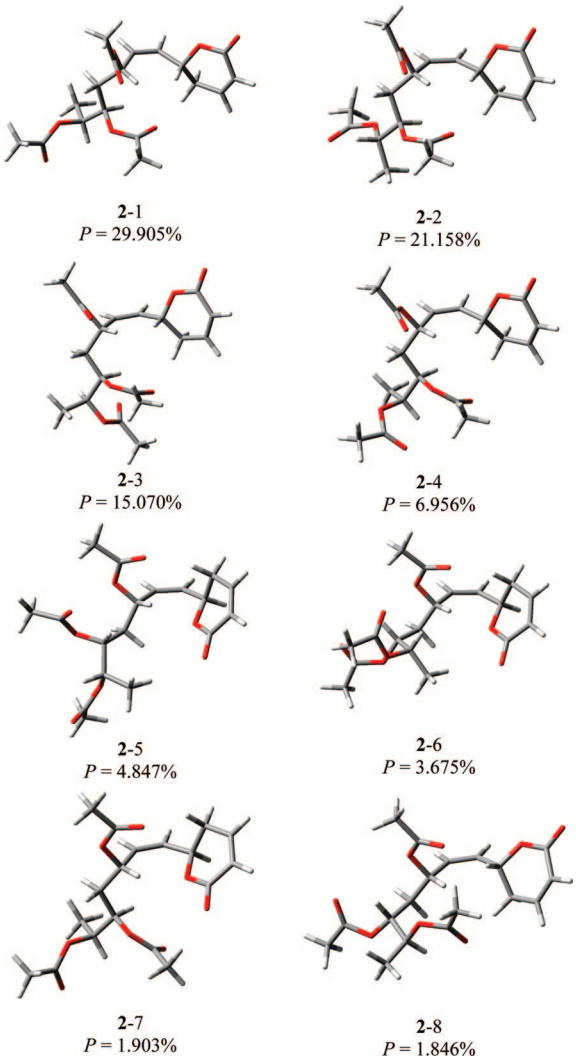

Figure 6. The eight most relevant conformers of **2** accounting for ca. 85% of the population.

Scheme 1. Synthesis of Tri-*O*-acetyl-3,6-dideoxy-D-glucose Diphenyldithioacetal (**14**)

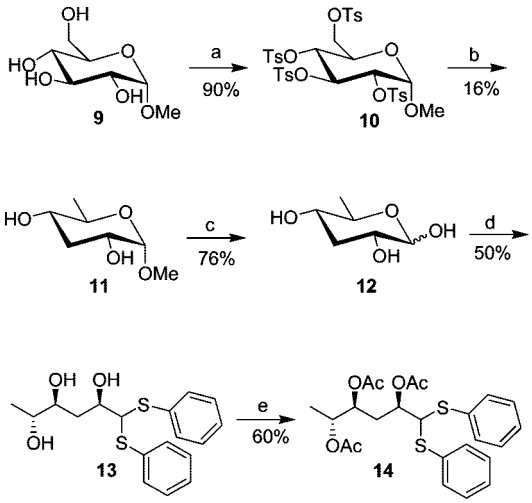

a) TsCl/pyridine; b) LAH/ether; c) HCl 1N;
d) $C_6H_5SH/Et_2O:BF_3$; e) Ac_2O/pyridine

in $CHCl_3$ on a Perkin-Elmer 16F PC FT spectrophotometer. EIMS data were obtained on a JEOL JMS-AX505HA mass spectrometer or on a Hewlett-Packard 5989A spectrometer. FABS were recorded on a JEOL DX300 mass spectrometer in the positive mode using NBA as the matrix. HRMS were measured at UCR Mass Spectrometry Facility, University of California, Riverside. Open column chromatography was carried out on Merck silica gel 60 (70−230 mesh ASTM) and TLC on Merck silica gel 60 F254 plates.

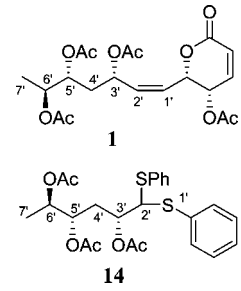

Figure 7. Comparison between the structure of **1** and tri-*O*-acetyl-3,6-dideoxy-D-glucose diphenyldithioacetal (**14**).

Table 5. Cytotoxicity Values (IC_{50} in μg/mL) for Hyptolide (**2**) and Spicigerolide (**3**)

compound	HEp-2	KB	HeLa
2	6.2	3.6	2.8
3	9.4	5.4[a]	15.9
ellipticine[b]	0.4	0.4	0.4

[a] Previously measured as 5.8 mg/mL.[6] [b] Employed as positive control.

Table 6. Cell Cycle Progression in Cervical Cancer (HeLa) Cells after 48 h Treatment with Hyptolide (**2**) and Spicigerolide (**3**) at a Concentration of $CI_{50} \times 10$[a]

compound	%G1	%S	%G2	rmsd
DMSO	41	42	14	0.086
2	34	57	7	0.062
3	40	34	23	0.112

[a] Percentage and rmsd values were obtained by using the Watson model.

NMR Data and Nonlinear Fit of the Spectra to Spectral Parameters. NMR spectra were measured in $CDCl_3$ solutions containing TMS as the internal standard at 300 MHz for ^{1}H and 75.4 MHz for ^{13}C on a Varian Mercury 300 spectrometer. Spectra were recorded at room temperature (22 °C) with a spectral width of 4.5 kHz and a digital resolution of 0.14 Hz/point. The data were subjected to Fourier transformation with zero filling to 64K points. The COSY spectrum for **14** was acquired with COSY 90-45 pulse sequence, a relaxation delay of 1 s, an acquisition time of 0.210 s, spectral width of 2438 Hz, 16 repetitions, and 256 increments in 1024 × 1024 data points, while the HETCOR experiment was carried out employing a relaxation delay of 1 s, acquisition time of 0.038 s, spectral width of 13 459 Hz, 2D width of 2528 Hz, 256 repetitions, and 256 increments in 2048 × 512 data points. Due to the lack of an authentic sample of **1**, the experimental coupling constants were obtained through nonlinear fit of the ^{1}H NMR spectrum to spectral parameters using spectral simulation based on the original ^{1}H NMR plot for this compound,[19] which was recorded at 300 MHz in $CDCl_3$ at room temperature on a Varian VXR-300 spectrometer with a spectral width of 4.5 kHz and a digital resolution of 0.14 Hz/point. ^{1}H NMR nonlinear fitting of the spectra for **1**, **2**, and **14** was obtained using the MestRe-C 3.0 program (Mestrelab Research, Santiago de Compostela, Spain).

Molecular Modeling Calculations. Molecular building and conformational search were carried out in the Spartan'04 program[41] using the MMFF94 force-field calculation on a Windows operating system machine. The conformational searching was performed through a Systematic Search protocol in which the torsion angles C(2′)−C(3′)−C(4′)−C(5′), C(3′)−C(4′)−C(5′)−C(6′), and C(4′)−C(5′)−C(6′)−C(7′) in the side chain were varied by 120°, starting at 60° for each central bond, and the torsion angles of the C(1′)═C(2′)−C(3′)−C(4′) and C(5)−C(6)−C(1′)═C(2′) dihedral angles were rotated in steps of 180°, generating a total of 108 initial conformers for each stereoisomer (**1a**−**1d**). The acetoxy moieties began at H−C_{sp^3}−O−C_{sp^2} and C_{sp^3}−O−C═O dihedral angles of ca. 0°, and conformational explorations for the acetyl groups

were achieved within dihedral angle ranges of +60° to −60°. Molecular potential energy of all structures was minimized to a rmsd gradient of 1×10^{-6} kcal/mol on the potential energy surface. An energy cutoff of 10 kcal/mol was selected in order to have a wide window of conformers in the Boltzmann distribution. All structures inside of the cutoff value were geometrically optimized using the hybrid DFT method B3LYP and basis set DGDZVP (B3LYP/DGDZVP). The optimized structures were used to calculate the thermochemical parameters, and the IR frequencies were estimated at 298 K and 1 atm. Magnetic shielding tensors were calculated with the gauge invariant atomic orbital method (GIAO), and $^1H-^1H$ vicinal coupling constants were obtained from the B3LYP/DGDZVP optimized structures using the SpinSpin option during the NMR job. All quantum mechanical, NMR, and optical rotation calculations were carried out using the Gaussian 03 program[42] on a Linux operating system in the KanBalam cluster from a Hewlett-Packard HP CP 4000, which includes 1368 AMD Opteron processors at 2.6 GHz and a RAM memory of 3 terabytes. Geometrical optimizations, frequencies, and coupling constant calculations for each stereoisomer required an approximate calculation time of 6450 h divided in 164 processors. Optical rotations required an additional calculation time of 418 h divided in 38 processors.

Methyl 2,3,4,6-Tetra-*O*-*p*-toluenesulfonyl-α-D-glucose (10). This compound was prepared from methyl α-D-glucopyranoside **9** as described previously.[34,43] Additional spectral data are as follows: ORD $[\alpha]_{589}$ +41 (lit.[43] +44.7), $[\alpha]_{578}$ +43, $[\alpha]_{546}$ +48, $[\alpha]_{436}$ +75, $[\alpha]_{365}$ +103 (*c* 0.80, $CHCl_3$); IR ($CHCl_3$) ν_{max} 2900, 1604, 1378, 1195, 1182, 1101, 1045, 979, 817 cm^{-1}; ^1H NMR (300 MHz, $CDCl_3$) δ 7.86−7.25 (16H, m, 4 OTs), 5.04 (1H, dd, $J_{2,3} = 9.8$; $J_{3,4} = 8.9$ Hz, H-3), 4.69 (1H, d, $J_{1,2} = 3.5$ Hz, H-1), 4.51 (1H, dd, $J_{3,4} = 8.9$; $J_{4,5} = 9.8$ Hz, H-4), 4.42 (1H, dd, $J_{5,6a} = 2.1$; $J_{6a,6b} = 11.3$ Hz, H-6a), 4.15 (1H, dd, $J_{1,2} = 3.5$; $J_{2,3} = 9.8$ Hz, H-2), 4.03 (dd, $J_{5,6b} = 6.6$; $J_{6a,6b} = 11.3$ Hz, H-6b), 3.93 (1H, ddd, $J_{4,5} = 9.8$ Hz, $J_{5,6a} = 2.1$, $J_{5,6b} = 6.6$, H-5), 3.21 (3H, s, OMe), 2.46 (3H, s, OTs), 2.44 (6H, s, 2 OTs), 2.43 (3H, s, OTs); ^{13}C NMR (75.4 MHz, $CDCl_3$) δ 145.7, 145.4, 145.0 (×2), 133.4, 132.8, 132.6, 132.3, 129.8 (×2), 129.8 (×2), 129.8 (×2), 129.6 (×2), 128.5 (×2), 128.4 (×2), 128.1 (×4), 96.4 (C-1), 75.2 (×2, C-2,3), 73.1 (C-4), 67.8 (C-6), 67.5 (C-5), 55.8 (OMe), 21.7 (OTs), 21.7 (×2 OTs), 21.7 (OTs); positive FAB-MS *m/z* 811 $[M + H]^+$ (4), 779 $[M - OMe]^+$ (2), 639 $[M - CH_3C_6H_4SO_3]^+$ (2), 607 $[M - CH_3C_6H_4SO_3 - OMe]^+$ (2), 481 (11), 281 (70), 155 (100); HRESI/APCIMS *m/z* 833.1029 (calcd for $C_{35}H_{38}O_{14}S_4$+Na, 833.1042).

Methyl 3,6-Dideoxy-α-D-*ribo*-hexapyranoside (11). Compound **10**[34,44] (5.0 g) was prepared as reported previously to afford **11** with identical yields, R_f, and $[\alpha]_D$. The ^1H NMR spectrum was in agreement with the partially reported data. ^1H NMR (300 MHz, $CDCl_3$) δ 4.61 (1H, d, $J_{1,2} = 3.7$ Hz, H-1), 3.72 (1H, ddd, $J_{1,2} = 3.7$, $J_{2,3e} = 4.6$, $J_{2,3a} = 11.4$ Hz, H-2), 3.51 (1H, dq, $J_{4,5} = 9.2$, $J_{5,6} = 6.2$ Hz, H-5), 3.44 (3H, s, OMe), 3.30 (1H, ddd, $J_{3e,4} = 4.6$, $J_{3a,4} = 11.6$, $J_{4,5} = 9.2$ Hz, H-4), 2.20 (1H, dt, $J_{2,3e} = J_{3e,4} = 4.6$, $J_{3e,3a} = 11.6$ Hz, H-3e), 1.64 (1H, q, $J_{2,3a} = J_{3e,3a} = J_{3a,4} = 11.6$ Hz, H-3a), 1.26 (3H, d, $J_{5,6} = 6.2$ Hz, Me-6); ^{13}C NMR (75.4 MHz, $CDCl_3$) δ 98.3 (C-1), 70.8 (C-4), 68.6 (C-5), 67.6 (C-2), 55.0 (MeO), 37.0 (C-3), 17.3 (C-6); EIMS *m/z* 162 $[M]^+$ (1), 131 $[M - OMe]^+$ (3), 118 (13), 74 (57), 58 (100), 43 (11).

3,6-Dideoxy-D-*ribo*-hexose (paratose) (12). A solution of methyl 3,6-dideoxy-α-D-*ribo*-hexapyranoside **11** (20 mg) in 1 N HCl (5 mL) was heated at 80 °C for 5 h. The solution was cooled, neutralized with saturated $NaHCO_3$ solution, evaporated to dryness, and purified by column chromatography on silica gel. Elution with EtOAc gave a syrup (14 mg, 76%), $R_f = 0.21$ (6:1 $CHCl_3$−MeOH), in agreement with reported data for paratose (**12**).[35,36]

Tri-*O*-acetyl-3,6-dideoxy-D-glucose Diphenyldithioacetal (14). A solution of paratose (**12**) (50 mg) and benzenethiol (0.15 mL) in 90% TFA (5 mL) was heated at 55 °C for 1 h. The reaction mixture was evaporated to dryness under an Ar flow, and the residue was purified by column chromatography on silica gel. Elution with CH_2Cl_2/MeOH (9:1) afforded diphenyldithioacetal **13** (60 mg), which was dissolved in pyridine (1 mL) and treated with Ac_2O (1 mL) at 4 °C. After 30 min, the reaction was quenched with ice and extracted with CH_2Cl_2. The organic layer was washed with diluted HCl, $NaHCO_3$-saturated solution, and H_2O, dried over $NaSO_4$, filtered, and evaporated under vacuum. The residue was purified by flash column chromatography eluting with hexane/ethyl acetate (7:3) to yield **14** (33 mg, 40%) as a colorless oil: ORD $[\alpha]_{589}$ −4, $[\alpha]_{578}$ −3, $[\alpha]_{546}$ −1, $[\alpha]_{436}$ +17, $[\alpha]_{365}$ +42 (*c* 0.20, $CHCl_3$); IR ($CHCl_3$) ν_{max} 3032, 2928, 1736, 1440, 1372, 1236, 1216, 1206, 784, 780, 772, 754, 692 cm^{-1}; ^1H NMR (300 MHz, $CDCl_3$) see Table 1; ^{13}C NMR (75.4 MHz, $CDCl_3$) δ 170.3, 170.2, 170.2 (3C=O), 133.7 (×2), 133.5 (×2), 132.2 (×2), 129.2 (×2), 129.1 (×2), 128.3, 128.0, 72.1 (C-3′), 71.3 (C-5′), 70.2 (C-6′), 61.9 (C-2′), 30.7 (C-4′), 21.1 (OAc), 20.8 (OAc), 20.7 (OAc), 15.0 (C-7′); EIMS *m/z* 476 $[M]^+$ (4), 367 $[M^+ - C_6H_5S]$ (79), 307 (92), 265 (82), 205 (100), 177 (28), 147 (23), 123 (36), 95 (18); HRESI/APCIMS *m/z* 499.1236 (calcd for $C_{24}H_{28}O_6S_2$+Na, 499.1225).

Cytotoxicity Assays. Human laryngeal carcinoma (HEp-2), human nasopharyngeal carcinoma (KB), and cervical cancer (HeLa) cells were maintained in RMPI 1640 medium with 10% fetal bovine serum and cultured at 37 °C in an atmosphere of 5% CO_2 in air (100% humidity). The cells at log phase of their growth cycle were treated in triplicate at various concentrations of the test samples (0.16−20.0 μg/mL) and incubated for 72 h at 37 °C in a humidified atmosphere of 5% CO_2. The cell concentrations were determined by the sulforhodamine B method.[45] Results were expressed as the dose that inhibits 50% control growth after the incubation period (ED_{50}).

Cell Cycle Evaluations. They were carried out according to standard procedures.[46] HeLa cells in logarithm phase were incubated for 48 h with hyptolide (**2**) or spicigerolide (**3**) ($IC_{50} \times 10$) in DMSO. Cells were fixed with cold EtOH 70% (v/v), stained for 12 h at 4 °C with triton X-100 (100 μL), trisodium citrate (100 mg), and RNase A (100 mg), and filtered through nylon mesh. The cell cycle analysis was performed in a Becton Dickinson FACSCalibur flow cytometer. Data analysis was carried out using the FlowJo program version 7.2.5.

Acknowledgment. Financial support (grant 45759-Q) was from Consejo Nacional de Ciencia y Tecnología. F.L.-V. received a posdoctoral fellowship from CONACyT (grant 45861-Q). Geometry optimizations and coupling constant calculations were performed in the HP Cluster Platform 4000 (KanBalam) at Departamento de Supercómputo, Dirección General de Servicios de Cómputo Académico, UNAM.

Supporting Information Available: Experimental and simulated ^1H NMR spectra of **2** and tri-*O*-acetyl-3,6-dideoxy-D-glucose diphenyldithioacetal (**14**). DFT B3LYP/DGDZVP free energies, population, and comparison between DFT and experimental $^1H-^1H$ coupling constants of stereoisomers **1b**−**1d**. DFT B3LYP/DGDZVP optical rotation of **1**. DFT atomic Cartesian coordinates for the more relevant conformers of **1** and **2**. This material is available free of charge via the Internet at http://pubs.acs.org.

References and Notes

(1) Huryn, D. M.; Wipf, P. In *Natural Product Chemistry and Anticancer Drug Discovery*; Neidle, S., Ed.; Cancer Drug Design and Discovery; Academic Press: New York, 2008; Part II, Chapter 5, pp 107−130.
(2) (a) Paull, K. D.; Lin, C. M.; Malspeis, L.; Hamel, E. *Cancer Res.* **1992**, *52*, 3892–3900. (b) Sarabia, F.; García-Castro, M.; Sánchez-Ruíz, A. *Curr. Bioact. Compd.* **2006**, *2*, 269–299.
(3) (a) Collett, L. A.; Davies-Coleman, M. T.; Rivett, D. E. A. In *Naturally Occurring 6-Substituted 5,6-Dihydro-α-Pyrones*; Herz, W., Falk, H., Kirby, G. W., Moore, R. E., Tamm, Ch., Eds.; Progress in the Chemistry of Organic Natural Products; Springer Verlag: New York, 1998; Vol. 75, pp 182−209. (b) Pereda-Miranda, R. In *Bioactive Natural Products from Traditionally Used Mexican Plants*; Arnason, J. T., Mata, R., Romeo, J. T.; Eds.; Phytochemistry of Medicinal Plants; Plenum:New York, 1995; pp 83−112.
(4) (a) Usui, T.; Watanabe, H.; Nakayama, H.; Tada, Y.; Kanoh, N.; Kondoh, M.; Asao, T.; Takio, K.; Watanabe, H.; Nishikawa, K.; Kitahara, T.; Osada, H. *Chem. Biol.* **2004**, *11*, 799–806. (b) Yoshida, M.; Matsui, Y.; Ikarashi, Y.; Usui, T.; Osada, H.; Wakasugi, H. *Anticancer Res.* **2007**, *27*, 729–736.
(5) Achmad, S.; Hoyer, T.; Kjaer, A.; Makmur, L.; Norrestam, R. *Acta Chem. Scand.* **1987**, *B41*, 599–609. (b) García-Fortanet, J.; Murga, J.; Carda, M.; Marco, J. A. *Tetrahedron* **2004**, *60*, 12261–12267.
(6) (a) Pereda-Miranda, R.; Fragoso-Serrano, M.; Cerda-García-Rojas, C. M. *Tetrahedron* **2001**, *57*, 47–53. (b) Falomir, E.; Murga, J.; Ruiz, P.; Carda, M.; Marco, J. A.; Pereda-Miranda, R.; Fragoso-Serrano, M.; Cerda-García-Rojas, C. M. *J. Org. Chem.* **2003**, *68*, 5672–5676.
(7) Pereda-Miranda, R.; Hernández, L.; Villavicencio, M. J.; Novelo, M.; Ibarra, P.; Chai, H.; Pezzuto, J. M. *J. Nat. Prod.* **1993**, *56*, 583–593.
(8) Lu, G. H.; Wang, F. P.; Pezzuto, J. M.; Tam, T. C. M.; Williams, I. D.; Che, C. T. *J. Nat. Prod.* **1997**, *60*, 425–427.
(9) Romo de Vivar, A.; Vidales, P.; Pérez, A. L. *Phytochemistry* **1991**, *30*, 2417–2418.

(10) Davis-Coleman, M. T., Rivett, D. E. A. In *Naturally Occurring 6-Substituted 5,6-Dihydro-α-Pyrones*; Herz, W., Falk, H., Kirby, G. W., Moore, R. E., Tamm, Ch., Eds.; Progress in the Chemistry of Organic Natural Products Springer; Verlag: New York, 1989; Vol. 55, pp 1−35.
(11) Alemany, A.; Márquez, C.; Pascual, C.; Valverde, S.; Perales, A.; Fayos, J.; Martínez-Ripoll, M. *Tetrahedron Lett.* **1979**, *37*, 3579–3582.
(12) (a) Hanessian, S. *Total Synthesis of Natural Products: The Chiron Approach*; Pergamon Press: Oxford, 1983; pp 7−39. (b) Lichtenthaler, F. W. In *Enantiopure Building Blocks from Sugars and their Utilization in Natural Product Synthesis*; Scheffold, R., Ed.; Modern Synthetic Methods; VCH Publishers: Weinheim, 1992; Chapter 6, pp 273−376.
(13) (a) Bagno, A.; Rastrelli, F.; Saielli, G. *Chem.−Eur. J.* **2006**, *12*, 5514–5525. (b) Manzo, E.; Gavagnin, M.; Bifulco, G.; Cimino, P.; Di Micco, S.; Ciavatta, M. L.; Guo, Y. W.; Cimino, G. *Tetrahedron* **2007**, *63*, 9970–9978. (c) Galasso, V.; Kovac, B.; Modelli, A. *Chem. Phys.* **2007**, *335*, 141–154. (d) Plaza, A.; Piacente, S.; Perrone, A.; Hamed, A.; Pizza, C.; Bifulco, G. *Tetrahedron* **2004**, *60*, 12201–12209.
(14) Stephens, P. J.; Pan, J. J.; Devlin, F. J.; Cheeseman, J. R. *J. Nat. Prod.* **2008**, *71*, 285–288.
(15) Cerda-García-Rojas, C. M.; Catalán, C. A. N.; Muro, A. C.; Joseph-Nathan, P. *J. Nat. Prod.* **2008**, *71*, 967–971.
(16) Grkovic, T.; Ding, Y.; Li, X. C.; Webb, V. L.; Ferreira, D.; Copp, B. R. *J. Org. Chem.* **2008**, *73*, 9133–9136.
(17) Ding, Y.; Li, X. C.; Ferreira, D. *J. Org. Chem.* **2007**, *72*, 9010–9017.
(18) Braddock, D. C.; Rzepa, H. S. *J. Nat. Prod.* **2008**, *71*, 728–730.
(19) Vidales Dávila, P. G. Estudio Químico-Biológico de Hyptis urticoides y Senecio toluccanus (Plantas con Propiedades Insecticidas) B.Sc. Thesis, Facultad de Química. Universidad Nacional Autónoma de México, Mexico City, México, 1990, p 85.
(20) Höltje, H. D.; Folkers, G. In *Molecular Modeling. Basic Principles and Applications*; Mannhold, R., Kubinyi, H., Timmerman, H., Eds.; Methods and Principles in Medicinal Chemistry; VCH: Weinheim, 1996; Vol. 5, pp 23−36.
(21) Mills, J. A. *Aust. J. Chem.* **1974**, *27*, 1433–1446.
(22) Osawa, E.; Imai, K.; Fujiyoshi-Yoneda, T.; Jaime, C.; Ma, P.; Masamune, S. *Tetrahedron* **1991**, *47*, 4579–4590.
(23) López-Calahorra, F.; Velasco, D.; Castells, J.; Jaime, C. *J. Org. Chem.* **1990**, *55*, 3530–3536.
(24) Hehre, W. J.; Radom, L.; Schleyer, P. V. R.; Pople, J. A. *Ab Initio Molecular Orbital Theory*; Wiley: New York, 1986.
(25) Haasnoot, C. A. G.; de Leeuw, F. A. A. M.; Altona, C. *Tetrahedron* **1980**, *36*, 2783–2792.
(26) Cerda-García-Rojas, C. M.; Zepeda, L. G.; Joseph-Nathan, P. *Tetrahedron Comp. Methodol.* **1990**, *3*, 113–118.
(27) (a) Halgren, T. *J. Comput. Chem.* **1996**, *17*, 490–519. (b) Halgren, T. *J. Comput. Chem.* **1996**, *17*, 520–552. (c) Halgren, T. *J. Comput. Chem.* **1996**, *17*, 553–586. (d) Halgren, T.; Nachbar, R. B. *J. Comput. Chem.* **1996**, *17*, 587–615. (e) Halgren, T. *J. Comput. Chem.* **1996**, *17*, 616–641.
(28) (a) Godbout, N.; Salahub, D. R.; Andzelm, J.; Wimmer, E. *Can. J. Chem.* **1992**, *70*, 560–571. (b) Andzelm, J.; Wimmer, E. *J. Chem. Phys.* **1992**, *96*, 1280–1303.
(29) (a) Deng, W.; Cheeseman, J. R.; Frisch, M. J. *J. Chem. Theory Comput.* **2006**, *2*, 1028–1037. (b) Peralta, J. E.; Scuseria, G. E.; Cheeseman, J. R.; Frisch, M. J. *Chem. Phys. Lett.* **2003**, *375*, 452–458. (c) Sychrovsky, V.; Grafenstein, J.; Cremer, D. *J. Chem. Phys.* **2000**, *113*, 3530–3547. (d) Helgaker, T.; Watson, M.; Handy, N. C. *J. Chem. Phys.* **2000**, *113*, 9402–9409.
(30) Wolinski, K.; Hilton, J. F.; Pulay, P. *J. Am. Chem. Soc.* **1990**, *112*, 8251–8260.
(31) Steinmetz, W. E.; Robustelli, P.; Edens, E.; Heineman, D. *J. Nat. Prod.* **2008**, *71*, 589–594.
(32) Steiner, T. *Angew. Chem., Int. Ed.* **2002**, *41*, 48–76.
(33) Desiraju, G. R. *Chem. Commun.* **2005**, 2995−3001.
(34) Ekborg, G.; Svensson, S. *Acta Chem. Scand.* **1973**, *27*, 1437–1439.
(35) Patroni, J. J.; Stick, V. R. *Aust. J. Chem.* **1978**, *31*, 445–446.
(36) Chmielewski, M. *Tetrahedron* **1980**, *36*, 2345–2352.
(37) (a) McCann, D. M.; Stephens, P. J.; Cheeseman, J. R. *J. Org. Chem.* **2004**, *69*, 8709–8717. (b) Stephens, P. J.; Devlin, F. J.; Cheeseman, J. R.; Frisch, M. J.; Rosini, C. *Org. Lett.* **2002**, *4*, 4595–4598.
(38) Stephens, P. J.; McCann, D. M.; Devlin, F. J.; Smith, A. B. *J. Nat. Prod.* **2006**, *69*, 1055–1064.
(39) Boalino, D. M.; Connolly, J. D.; McLean, S.; Reynolds, W. F. *Phytochemistry* **2003**, *64*, 1303–1307.
(40) García-Fortanet, J.; Murga, J.; Carda, M.; Marco, J. A. *Arkivoc* **2005**, *9*, 175–188.
(41) Kong, J.; White, C. A.; Krylov, A. I.; Sherrill, C. D.; Adamson, R. D.; Furlani, T. R.; Lee, M. S.; Lee, A. M.; Gwaltney, S. R.; Adams, T. R.; Ochsenfeld, C.; Gilbert, A. T. B.; Kedziora, G. S.; Rassolov, V. A.; Maurice, D. R.; Nair, N.; Shao, Y.; Besley, N. A.; Maslen, P. E.; Dombroski, J. P.; Daschel, H.; Zhang, W.; Korambath, P. P.; Baker, J.; Byrd, E. F. C.; Van Voorhis, T.; Oumi, M.; Hirata, S.; Hsu, C.-P.; Ishikawa, N.; Florian, J.; Warshel, A.; Johnson, B. G.; Gill, P. M. W.; Head-Gordon, M.; Pople, J. A. *J. Comput. Chem.* **2000**, *21*, 1532–1548.
(42) Frisch, M. J.; Trucks, G. W.; Schlegel, H. B.; Scuseria, G. E.; Robb, M. A.; Cheeseman, J. R.; Montgomery, J. A., Jr.; Vreven, T.; Kudin, K. N. ; Burant, J. C.; Millam, J. M.; Iyengar, S. S.; Tomasi, J.; Barone, V.; Mennucci, B.; Cossi, M.; Scalmani, G.; Rega, N.; Petersson, G. A.; Nakatsuji, H.; Hada, M.; Ehara, M.; Toyota, K.; Fukuda, R.; Hasegawa, J.; Ishida, M.; Nakajima, T.; Honda, Y. ; Kitao, O.; Nakai, H.; Klene, M.; Li, X.; Knox, J. E.; Hratchian, H. P.; Cross, J. B.; Bakken, V.; Adamo, C.; Jaramillo, J.; Gomperts, R.; Stratmann, R. E.; Yazyev, O.; Austin, A. J. ; Cammi, R. ; Pomelli, C.; Ochterski, J. W. ; Ayala, P. Y.; Morokuma, K.; Voth, G. A.; Salvador, P.; Dannenberg, J. J.; Zakrzewski, V. G.; Dapprich, S.; Daniels, A. D.; Strain, M. C.; Farkas, O.; Malick, D. K.; Rabuck, A. D.; Raghavachari, K.; Foresman, J. B.; Ortiz, J. V.; Cui, Q.; Baboul, A. G.; Clifford, S.; Cioslowski, J.; Stefanov, B. B.; Liu, G.; Liashenko, A.; Piskorz, P.; Komaromi, I.; Martin, R. L.; Fox, D. J.; Keith, T.; Al-Laham, M. A.; Peng, C. Y.; Nanayakkara, A.; Challacombe, M.; Gill, P. M. W.; Johnson, B. ; Chen, W.; Wong, M. W.; Gonzalez, C.; Pople, J. A. *Gaussian 03*; Gaussian, Inc.: Wallingford, CT, 2004.
(43) Hess, K.; Stenzel, H. *Chem. Ber.* **1935**, *68B*, 981–989.
(44) Klausener, A.; Runsink, J.; Scharf, H. D. *Ann. Chem.* **1984**, 783−790.
(45) (a) Skehan, P.; Storeng, R.; Scudiero, D.; Monks, A.; McMahon, J.; Vistica, D.; Warren, J. T.; Bokesch, H.; Kenney, S.; Boyd, M. R. *J. Natl. Cancer Inst.* **1990**, *82*, 1107–1112. (b) Angerhofer, C. K.; Guinaudeau, H.; Wongpanich, V.; Pezzuto, J. M.; Cordell, G. *J. Nat. Prod.* **1999**, *62*, 59–66.
(46) Nunez, R. *Curr. Issues Mol. Biol.* **2001**, *3*, 67–70.

NP800447K